Cornelia Denz
Sergej Flach
Yuri S. Kivshar
Editors

SPRINGER SERIES IN OPTICAL SCIENCES 150

Nonlinearities in Periodic Structures and Metamaterials

Springer

10

Transporting Cold Atoms in Optical Lattices with Ratchets: Mechanisms and Symmetries

Sergey Denisov[1], Sergej Flach[2], and Peter Hänggi[1]

[1] Institut für Physik, Universität Augsburg, Universitätsstr. 1, 86135 Augsburg, Germany
sergey.denisov@physik.uni-augsburg.de, hanggi@physik.uni-augsburg.de
[2] Max-Planck-Institut für Physik Komplexer Systeme, Nöthnitzer Str. 38, 01187 Dresden, Germany
flach@mpipks-dresden.mpg.de

10.1 Introduction

Thermal fluctuations alone cannot create a steady directed transport in an unbiased system. However, if a system is out of equilibrium, the Second Law of Thermodynamics no longer applies, and then there are no thermodynamical constraints on the appearance of a steady transport [1, 2]. A directed current can be generated out of a fluctuating (time-dependent) external field with zero mean. The corresponding *ratchet effect* [3–9] has been proposed as a physical mechanism of a microbiological motility more then a decade ago [4,5]. Later on the ratchet idea has found diverse applications in different areas [6–9], from a molecular nanoscale-machine [10] up to quantum systems and quantum devices [11–17].

When the deviation from an equilibrium regime is small (the case of weak external fields) one may use the linear response theory in order to estimate the answer of the system [18–20]. However, due to the linearization of the response, the current value will be strictly zero since the driving field has zero bias. Therefore, one has to take into account nonlinear corrections and then derive the corresponding nonlinear response functional [20, 21], which may become a very complicated task, if the nonadiabatic regime is to be considered.

To obtain a dc-current, one has to break certain discrete symmetries, which involve simultaneous transformations in space and time. A recently elaborated *symmetry approach* [22, 23] established a clear relationship between the appearance of a directed current and broken space-time symmetries of the *equations of motion*. Thus, the symmetry analysis provides an information about the conditions for a directed transport appearance without the necessity of considering a nonlinear response functional.

Most theoretical and experimental studies have focused on ratchet realizations at a noisy overdamped limit [6–9]. However, systematic studies of the underlying broken symmetries, and the largest possible values of directed currents achieved for different dissipation strength, show that the dc current values typically become orders of magnitude larger in the limit of weak dissipation [24,25]. The corresponding dynamics is characterized by long space-time correlations which may drastically increase the rectification efficiency [25,26].

Fast progress in experimental studies of cold atoms ensemble dynamics have provided clean and versatile experimental evidence of a ratchet mechanism in the regime of weak or even vanishing dissipation [27,28]. The results of the corresponding symmetry analysis for the regime of classical dynamics has already been successfully tested with cold Rubidium and Cesium atoms in optical lattices with a tunable weak dissipation [29–32]. Further decreasing of the dissipation strength leads to the quantum regime [27]. Recent experiments have shown the possibility to achieve an optical lattice with tunable asymmetry in the quantum regime [33]. A Bose-Einstein condensate (BEC) loaded into an optical potential is another candidate for a realization of quantum ratchets in the presence of atom-atom interactions [28]. While there is obvious interest in experimental realizations of theoretically predicted symmetry broken states, another important aspect of the interface between cold atoms and the ratchet mechanism is, that new possibilities for a control of the dynamics of atomic systems by laser fields may be explored [34,35].

The objective of this work is to provide a general introduction into the symmetry analysis of the rachet effect using a simple, non-interacting one-particle dynamics. Despite its simplicity, this model contains all the basic aspects of classical and quantum ratchet dynamics, and may be used also as a starting point of incorporating atom-atom interactions.

10.2 Single Particle Dynamics

We start with the simple model of an underdamped particle with mass m, moving in a space-periodic potential $U(x) = U(x + \lambda)$ under the influence of the external force $\chi(t)$ with zero mean:

$$m\ddot{x} + \gamma\dot{x} - f(x) - \chi(t) = 0\,. \tag{10.1}$$

Here $f(x) = -U'(x)$, $\int_0^\lambda f(x)\,\mathrm{d}x = 0$, and γ is the friction coefficient. Next, we ask whether a directed transport with nonzero mean velocity, $\langle\dot{x}\rangle \neq 0$, may appear in the system (10.1).

If $\chi(t) \equiv \xi(t)$ is a realization of a Gaussian white (i.e. delta-correlated) noise, obeying via its correlation properties the (second) fluctuation-dissipation theorem [20], Eq. (10.1) then describes the thermal equilibrium state of a particle interacting with a heat bath. From the Second Law of Thermodynamics it follows that a directed transport is absent, independently of the particular choice of the periodic potential $U(x)$ [4,6,7,24].

The presence of temporary correlations in $\chi(t)$ may change the situation drastically. A simple way to get such correlations is to use an additive periodic field $E(t)$,

$$\chi(t) = \xi(t) + E(t) , \qquad E(t) = E(t+T) , \qquad \int_0^T E(t)\,\mathrm{d}t = 0 . \tag{10.2}$$

If $\xi(t)$ is a realization of a white noise, then the functions $-\xi(t)$, $\xi(t)$, and $\xi(t+\tau)$ are also realizations of the same white noise, and their statistical weights are equal to the statistical weight of the original realization. For what comes, the noise term $\xi(t)$ will thus not be relevant for the following symmetry analysis. We consider the symmetries of the deterministic differential equation

$$m\ddot{x} + \gamma\dot{x} - f(x) - E(t) = 0 . \tag{10.3}$$

Eq. (10.3) contains two periodic functions, $f(x)$ and $E(t)$, both with zero mean. The properties of the symmetries of the Eq. (10.3) are strongly depending on the symmetry properties of these functions.

10.3 Symmetries

10.3.1 Symmetries of a Periodic Function with Zero Mean

Let us consider a periodic function $g(z + 2\pi) = g(z)$ with zero mean, $\int_0^{2\pi} g(z)\,\mathrm{d}z = 0$. This function can be expanded into a Fourier series

$$g(z) = \sum_{k=-\infty}^{\infty} g_k \cdot \exp(\mathrm{i}kz) , \tag{10.4}$$

where $g_0 \equiv 0$. We will consider real-valued functions; therefore, $g_k = g^*_{-k}$.

The function $g(z)$ may possess three different symmetries. First, it can be *symmetric*, $g(z + z_0) = g(-z + z_0)$, around a certain argument value z_0. For such functions we will use the notation g_s. The Fourier expansion (10.4) contains, after the shift by z_0, only cosine terms, so $g_k(z_0) = g_k \cdot \exp(\mathrm{i}kz_0)$ are real numbers, i.e. $g_k(z_0) = g_{-k}(z_0)$.

Second, the function $g(z)$ can be *antisymmetric*, $g(z + z_1) = -g(-z + z_1)$, around a certain value of the argument, z_1. For such functions we will use the notation g_a. The corresponding Fourier expansion (10.4) contains only sine terms (after the shift by z_1), so $g_k(z_0) = g_k \cdot \exp(\mathrm{i}kz_0)$ are pure imaginary numbers, and $g_k(z_0) = -g_{-k}(z_0)$.

Finally, the function $g(z)$ can be *shift-symmetric*, $g(z) = -g(z + \pi)$. The Fourier expansion of a shift-symmetric function $g_\mathrm{sh}(z)$ contains odd harmonics only, $g_{2m} \equiv 0$.

It is straightforward to show that a periodic function $g(z)$ can have either none of the above mentioned symmetries, or exactly one of them, or all three of

them. Let us consider several simple examples. The function $\cos(z)$ possesses all three symmetries. The function $\cos(z)+\cos(3\,z+\phi)$ always possesses shift-symmetry and in addition may be simultaneously symmetric and antisymmetric for $\phi = 0, \pm\pi$. The function $\cos(z)+\cos(2\,z+\phi)$ is not shift-symmetric, thus it will either have no other symmetry at all, except for $\phi = 0, \pm\pi$ (symmetric), and $\phi = \pm\pi/2$ (antisymmetric).

10.3.2 Symmetries of the Equations of Motion

The system dynamics in Eq. (10.3) can be described by three first-order autonomous differential equations,

$$\dot{x} = \frac{p}{m}\,, \qquad \dot{p} = f(x) + E(\tau) - \frac{\gamma}{m}p\,, \qquad \dot{\tau} = 1\,. \tag{10.5}$$

The phase-space dimension is three. We are looking for symmetrytransformations $\hat{S}$, which do not change the equation (10.5), but do change the sign of the velocity $\dot{x}$. Such transformations map the phase space $\{x, p, \tau\}$ onto itself. If we find such a transformation, we then apply it to all points of a given trajectory. We get a new manifold in phase space, which also represents a trajectory, i.e., a solution of the equations (10.5). The original trajectory and its image may coincide (or may not).

Let us assume that we have found such a transformation. Next, we consider the mean velocity, $\bar{v} = \lim_{s\to\infty}(x(t_0+s)-x(t_0))/s$, on the original trajectory. If the trajectory and its image coincide, then $\bar{v} = 0$. If they are different then their velocities have the same absolute value but opposite signs. If, in addition, both the trajectories have the same statistical weights in the presence of a white noise, then we can conclude that the average current in the system (10.3) is equal to zero [22].

There are only two possible types of transformations which change the sign of the velocity $\dot{x}$: they include either a time-reversal operation, $t \to -t$, or a space inversion, $x \to -x$ (but not both operations simultaneously!).

The following symmetries can be identified [22]:

$$\begin{aligned}
\hat{S}_{\rm a} &: \quad x \to -x\,, \quad t \to t + \frac{T}{2}\,, \quad \text{if } \{f_{\rm a}, E_{\rm sh}\}\,, \\
\hat{S}_{\rm b} &: \quad x \to x\,, \quad t \to -t\,, \quad \text{if } \{E_{\rm s}, \gamma = 0\}\,, \\
\hat{S}_{c} &: \quad x \to x + \frac{\lambda}{2}\,, \quad t \to -t\,, \quad \text{if } \{f_{\rm sh}, E_{\rm a}, m = 0\}\,.
\end{aligned} \tag{10.6}$$

The symmetry $\hat{S}_{\rm b}$ requires zero dissipation, $\gamma = 0$, i.e., it requires the Hamiltonian regime, and the symmetry $\hat{S}_{\rm c}$ can be fulfilled in the overdamped limit (i.e. $m = 0$) only. Note that all symmetries require certain symmetry properties of the function $E(t)$. Usually, an experimental setup allows to tune the shape of the time-dependent field $E(t)$ easier than the shape of the spatially periodic potential [36,37]. A proper choice of the force $E(t)$ may break all three

symmetries for any coordinate dependence of the force $f(x)$. We restrict the further consideration to the case of a symmetric potential $U(x) = 1 - \cos(x)$ while using a bi-harmonic driving force,

$$E(t) = E_1 \cos(t) + E_2 \cos(2\,t + \theta) \;, \tag{10.7}$$

for a symmetry violation. If $\theta \neq 0, \pi/2, \pi, 3\,\pi/2$ then all three symmetries (10.6) are broken and we may count on a nonzero mean velocity, $v \neq 0$.

10.3.3 The Case of Quasiperiodic Functions

We generalize the symmetry analysis to the case of quasiperiodic driving field $E(t)$ [38,39].

We consider a quasiperiodic function $g(z)$ to be of the form

$$g(z) \equiv \tilde{g}(z_1, z_2, \ldots, z_N) \;, \qquad \frac{\partial z_i}{\partial z} = \Omega_i \tag{10.8}$$

where all ratios Ω_i/Ω_j are irrational if $i \neq j$ and $\tilde{g}(z_1, z_2, \ldots, z_i + 2\,\pi, \ldots, z_N) = \tilde{g}(z_1, z_2, \ldots, z_i, \ldots, z_N)$ for any i. Such a function may have numerous symmetries. With respect to the following symmetry analysis of the equation of motion we will list here only those symmetries of $\tilde{g}$ which are of relevance. It can be symmetric $\tilde{g}_{\rm s}(z_1, z_2, \ldots, z_N) = \tilde{g}_{\rm s}(-z_1, -z_2, \ldots, -z_N)$, antisymmetric $\tilde{g}_{\rm a}(z_1, z_2, \ldots, z_N) = -\tilde{g}_{\rm a}(-z_1, -z_2, \ldots, -z_N)$. It can be also shift-symmetric for a given set of indices $\tilde{g}_{{\rm sh},\{i,j,\ldots,m\}}$ which means that $\tilde{g}$ changes sign when a shift by π is performed in the direction of each $z_i, z_j, \ldots, z_m$ only, leaving the other variables unchanged.

The relevant symmetry properties of $\tilde{g}$ are thus studied on the compact space of variables $\{z_1, z_2, \ldots, z_N\}$. The irrationality of the frequency ratios guarantees that in the course of evolution of z this compact space is densely scanned by these variables with uniform density in the limit of large z. At the same time we note that it is always possible to find a large enough value Z such that

$$\lim_{\tau \to \infty} \frac{1}{\tau} \int_0^\tau \left(g(z + Z) - g(z)\right)^2 \, {\rm d}z < \epsilon \tag{10.9}$$

with (arbitrarily) small absolute value of ϵ. For a given value of ϵ this defines a quasiperiod Z of the function $g(z)$.

In order to make the symmetry analysis of the equation of motion transparent, we rewrite it (skipping the noise term) in the following form [39]:

$$\begin{aligned} m\ddot{x} + \gamma\dot{x} - f(x) - E(\phi_1, \phi_2, \ldots, \phi_N) &= 0 \;, \\ \dot{\phi}_1 &= \omega_1 \;, \\ \dot{\phi}_2 &= \omega_2 \;, \\ &\vdots \\ \dot{\phi}_N &= \omega_N \;. \end{aligned} \tag{10.10}$$

The function $f(x)$ is also assumed to be quasiperiodic with M corresponding spatial frequencies.

The following symmetries can be identified, which change the sign of $\langle \dot{x} \rangle$ and leave (10.10) unchanged:

$$\begin{aligned} \tilde{S}_{\mathrm{a}} &: \quad x \to -x\,, \quad \phi_{i,j,\ldots,m} \to \phi_{i,j,\ldots,m} + \pi\,, \quad \text{if } \{f_{\mathrm{a}}, E_{\mathrm{sh},\{i,j,\ldots,m\}}\}\,, \\ \tilde{S}_{\mathrm{b}} &: \quad x \to x\,, \quad t \to -t\,, \quad \text{if } \{E_{\mathrm{s}}, \gamma = 0\}\,, \\ \tilde{S}_{\mathrm{c}} &: \quad x \to x + \frac{\lambda}{2}\,, \quad t \to -t\,, \quad \text{if } \{f_{\mathrm{sh},\{1,2,3,\ldots,M\}}, E_{\mathrm{a}}, m = 0\}\,. \end{aligned} \tag{10.11}$$

The symmetry $\tilde{S}_{\mathrm{a}}$ is actually a set of various symmetry operations which are defined by the given subset of indices $\{i, j, \ldots, m\}$.

The prediction then is, that if for a given set of parameters any of the relevant symmetries (10.11) is fulfilled, the average current will be zero. If however the choice of functions $f(x)$ and $E(t)$ is such that the symmetries are violated, a nonzero current is expected to emerge.

10.4 Dynamical Mechanisms of Rectification: The Hamiltonian Limit

Let us consider the limit $\gamma = 0$ (Hamiltonian case) [22, 26]. Due to time and space periodicity of the system (10.3) we can map the original three-dimensional phase space (x, p, t) onto a two-dimensional cylinder, $\mathcal{T}^2 = (x \mod 1, p)$, by using the stroboscopic Poincaré section after each period $T = 2\pi/\omega$. For given initial conditions $\{x(0), p(0)\}$, we integrate the system over time T, and then plot the final point, $\{x(T), p(T)\}$, on the cylinder $\mathcal{T}^2$.

For $E(t) = 0$ the system (10.3) is integrable and there is a separatrix in the phase space which separates oscillating and running solutions. A non-zero field $E(t)$ destroys the separatrix and leads to the appearance of a stochastic layer (see Fig. 10.1). In this part of the phase space the system dynamics is ergodic, i.e., all average characteristics are the same for all trajectories, launched inside the layer. Therefore, the symmetry analysis is valid for all trajectories on this manifold. Numerical studies have confirmed this conclusion [22, 23, 26]. Fig. 10.2 shows several trajectories $x(t)$ from chaotic layers and illustrates the fact that the violation of symmetries causes a directed motion of the particle.

The dynamics within the stochastic layer can be roughly subdivided into two distinct fractions. The first one corresponds to ballistic flights near the layer boundaries. They appear due to a sticking effect [40]. A random diffusion within a chaotic bulk is attributed to the second fraction. A rectification effect appears due to a violation of the balance between ballistic flights in opposite directions [26]. This interpretation supports the view, that even in the presence of damping and noise, the ratchet mechanism relies on harvesting on temporal correlations of the underlying dynamical system. Ballistic flights are just such examples of long temporal correlations on a trajectory which

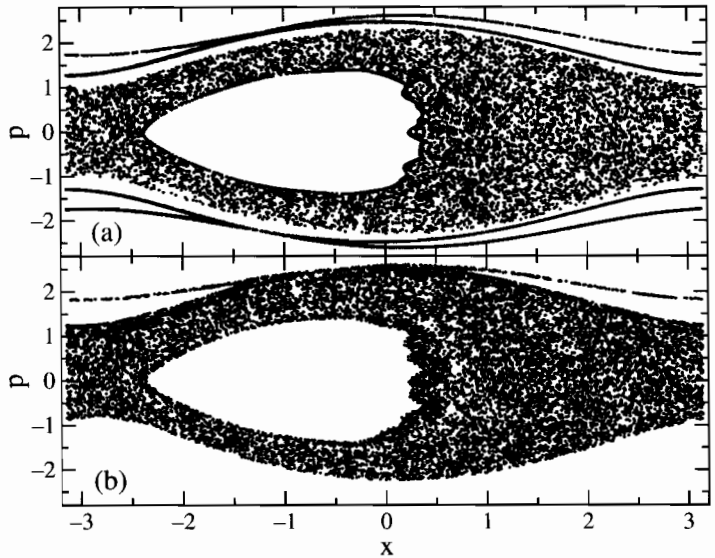

Fig. 10.1. Poincaré map for the system (10.5), (10.7). The parameters are $E_1 = 0.252$, $E_2 = 0.052$, $\gamma = 0$. (**a**) $\theta = 0$, (**b**) $\theta = \pi/2$

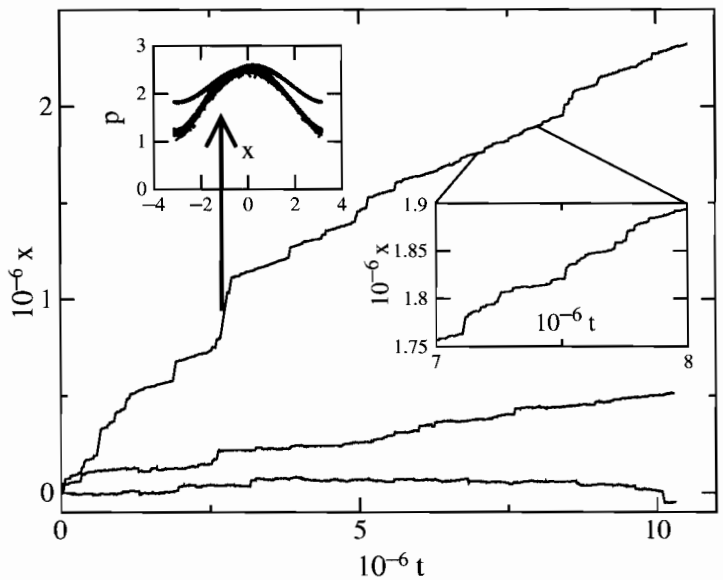

Fig. 10.2. $x(t)$ for $\theta = 0, \pi/5, \pi/2$ (lower, middle and upper curves, respectively). Left upper inset: Poincaré map for a single ballistic flight, $\theta = \pi/2$. Right inset: zoom of $x(t)$ for the case $\theta = \pi/2$

is overall chaotic. Therefore it is not surprising, that the ratchet effect is stronger in the dissipationless limit, since dissipation will introduce finite (and possibly short) time scales which cut the temporal correlations down. The averaged drift velocity can be estimated by using a sum rule [41, 42]. From the corresponding approach, which is based on a statistical argument by the authors of Ref. [41, 42], it follows, that a mixed space, i.e., a stochastic layer with boundaries and embedded regular submanifolds (islands), presents the necessary condition for a directed transport.

The adding of a non-zero dissipation, $\gamma \neq 0$, does not change the situation drastically [23]. The symmetry analysis is still valid for this case. The phase space is shared by different transporting and non-transporting attractors with their corresponding basins of attraction, which are strongly entangled inside the former stochastic layer region. A symmetry violation causes a desymmetrization of basins. Finally, a weak noise leads to a trajectory wandering over different basins, sticking to corresponding attractors, and, finally, to the rectification effect. The long flights which appear at the Hamiltonian limit are damped after a characteristic time which is the shorter, the larger the dissipation strength γ is [23, 26].

A systematic analysis shows that, under the condition of full symmetry violation, the approach of the dissipationless limit leads to a drastic increase of the dc current value [25], which depends on the characteristics of the stochastic layer [26]. It has been shown that, in a full accordance with the symmetry analysis, the dc current disappears near $\theta = 0, \pi$ for the case of weak dissipation, and near $\theta = \pm\pi/2$ at the strong dissipation limit. The value of the phase θ, at which the current becomes zero, is a monotonous function of the dissipation strength γ [25].

An inclusion of a dc-component to the external field, $\tilde{E}(t) = E(t) + E_{\mathrm{dc}}$, may lead to a directed transport against a constant bias E_{dc}, even in the Hamiltonian limit [43].

The abovementioned results have been confirmed in cold atoms experiments, performed in the group of Renzoni [29–31]. In these experiments, atoms of Cs and Rb have been cooled to temperatures of several mK. An optical standing wave, created by a pair of counter-propagating laser beams, formed a periodic potential for the atoms. Finally, a time-dependent force $E(t)$ has been introduced through a periodic modulation of the phase for one of the beams. The results of the above symmetry analysis have been verified by changing the relative phase ϕ and by tuning the effective dissipation strength.

The case of the quasiperiodic driving force $E(t)$ for cold atoms ratchets also has been studied experimentally [32], with a similar outcome.

10.5 Resonant Enhancement of Transport with Quantum Ratchets

A quantum extension of the (dissipationless) system dynamics in Eq. (10.3) can readily be achieved [44,45]. The system evolution can be described by the Schrödinger equation,

$$\mathrm{i}\hbar\frac{\partial}{\partial t}|\psi(t)\rangle = H(t)|\psi(t)\rangle \;, \tag{10.12}$$

where the Hamiltonian H is of the form

$$H(x,p,t) = \frac{p^2}{2} + [1+\cos(x)] - xE(t) \;. \tag{10.13}$$

The system (10.12) describes a cloud of noninteracting atoms, placed into a periodic potential (formed by two counter-propagating laser beams) and exposed to an external ac field (10.7)[1].

Because of the time and space periodicity of the Hamiltonian (10.13), the solutions $|\psi_\alpha(t+t_0)\rangle = U(t,t_0)|\psi_\alpha(t_0)\rangle$ of the Schrödinger equation (10.12) can be characterized by the eigenfunctions of the Floquet operator $U(T,t_0)$ which satisfy the Floquet theorem $|\psi_\alpha(t)\rangle = \exp(-\mathrm{i}E_\alpha t/T)|\phi_\alpha(t)\rangle$, $|\phi_\alpha(t+T)\rangle = |\phi_\alpha(t)\rangle$ (here t_0 is the initial time). The quasienergies E_α ($-\pi < E_\alpha < \pi$) and the Floquet eigenstates can be obtained as solutions of the eigenvalue problem of the Floquet operator

$$U(T,t_0)|\phi_\alpha(t_0)\rangle = \mathrm{e}^{-\mathrm{i}E_\alpha}|\phi_\alpha(t_0)\rangle \tag{10.14}$$

with α denoting the band index and with k being the wave vector [44–47]. An initial state can be expanded over Floquet-Bloch eigenstates, $|\psi(t_0)\rangle = \sum_{\alpha,k} C_{\alpha,k}(t_0)|\phi_{\alpha,k}\rangle$ and the subsequent state's evolution is encoded in the coefficients $\{C_{\alpha,k}\}$. We restrict further consideration to the case $\kappa = 0$ which corresponds to initial states where atoms equally populate all (or many) wells of the spatial potential.

The mean momentum expectation value,

$$J(t_0) = \lim_{t\to\infty}\frac{1}{t}\int_{t_0}^{t}\langle\psi(\tau,t_0)|\hat{p}|\psi(\tau,t_0)\rangle\,\mathrm{d}\tau \;, \tag{10.15}$$

measures the asymptotic current. Expanding the wave function over the Floquet states the current becomes

$$J(t_0) = \sum_\alpha \langle p\rangle_\alpha |C_\alpha(t_0)|^2 \;, \tag{10.16}$$

where $\langle p\rangle_\alpha$ is the mean momentum of the Floquet state $|\phi_\alpha\rangle$ [44–46].

[1] The dissipation may be included into quantum dynamics by coupling the system (10.13) to a heat bath, $H_{\mathrm{diss}}(x,p,t,\{\boldsymbol{q}\}) = H(x,p,t) + H_{\mathrm{B}}(x,\{\boldsymbol{q}\})$. Here $H_{\mathrm{B}}(x,\{\boldsymbol{q}\})$ describes an ensemble of harmonic oscillators $\{\boldsymbol{q}\}$ at thermal equilibrium interacting with the system [11].

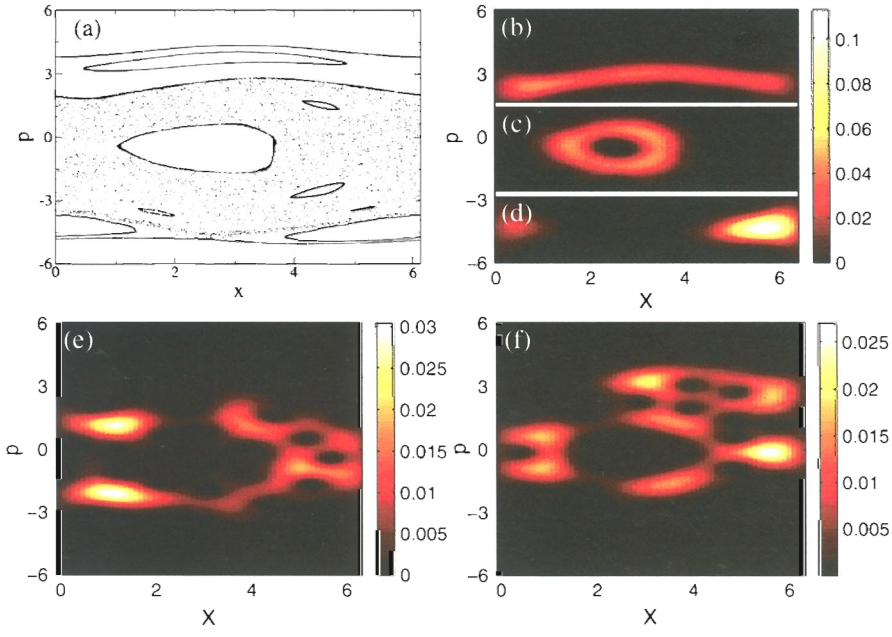

Fig. 10.3. (**a**) Poincaré section for the classical limit, (10.7), (10.13), (**b**)–(**f**) Husimi representations for different Floquet eigenstates for the Hamiltonian (10.13) with $\hbar = 0.2$ (momentum is in units of the recoil momentum, $p_r = \hbar k_L$, with $k_L = 1$). The parameters are $E_1 = E_2 = 2$, $\omega = 2$, $\theta = -\pi/2$ and $t_0 = 0$ for (b)–(e), and $E_1 = 3.26$, $E_2 = 1$, $\omega = 3$, $\theta = -\pi/2$ and $t_0 = 0$ for (f)

The analysis of the transport properties of the eigenstates shows that the quantum system inherits the symmetries of its classical counterpart [44,45]. In particular, the symmetries of the classical equations of motion translate into symmetries of the Floquet operator. The presence of any of these symmetries results in a vanishing the time-averaged expectation value of the momentum operator for each Floquet eigenstate: $\langle p \rangle_\alpha = 0$. Thus, if one of the symmetries, $\tilde{S}_a$, $\tilde{S}_b$ (10.11), holds then $\langle p \rangle_\alpha = 0$ for all α. Consequently $J(t_0) = 0$ in this case.

By using the Husimi representation [48,49] we can visualize different eigenstates in the phase space, $\{x, p, \tau\}$ and establish a correspondence between them and the mixed phase space structures for the classical limit (Fig. 10.3).

Since the Schrödinger equation (10.12) is linear, the system maintains a memory of the initial condition for infinite times [50]. The asymptotic current value depends on the initial time, t_0, and on the initial wave function, $\psi(t_0)$. For a given initial wave function, $|\psi\rangle = |0\rangle$, we can assign a unique current value by performing an averaging over the initial time t_0, $J = 1/T \int_0^T J(t_0)\, \mathrm{d}t_0$ [44,45]. Fig. 10.4 shows the dependence of the average

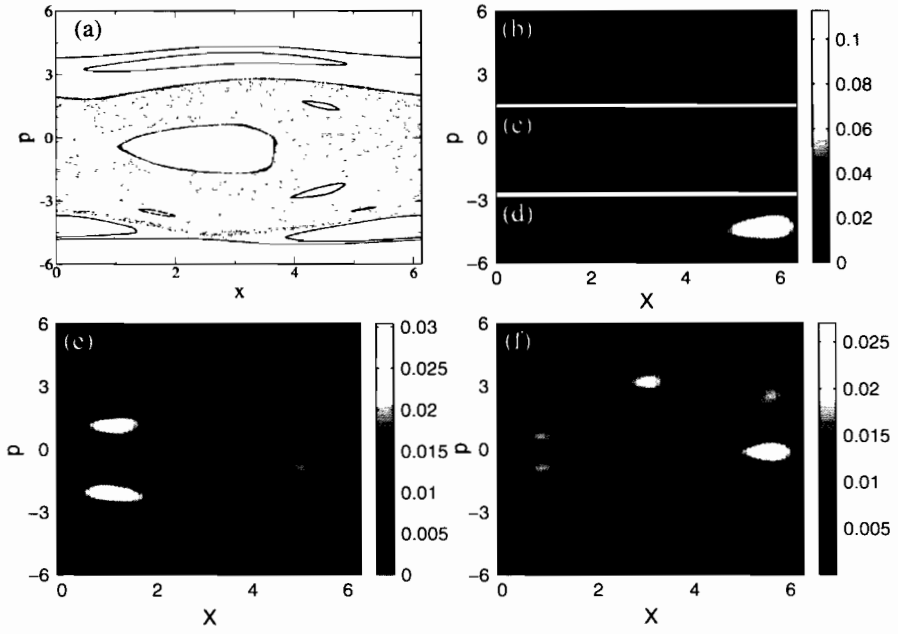

Fig. 10.3. (**a**) Poincaré section for the classical limit, (10.7), (10.13), (**b**)–(**f**) Husimi representations for different Floquet eigenstates for the Hamiltonian (10.13) with $\hbar = 0.2$ (momentum is in units of the recoil momentum, $p_r = \hbar k_L$, with $k_L = 1$). The parameters are $E_1 = E_2 = 2$, $\omega = 2$, $\theta = -\pi/2$ and $t_0 = 0$ for (b)–(e), and $E_1 = 3.26$, $E_2 = 1$, $\omega = 3$, $\theta = -\pi/2$ and $t_0 = 0$ for (f)

The analysis of the transport properties of the eigenstates shows that the quantum system inherits the symmetries of its classical counterpart [44,45]. In particular, the symmetries of the classical equations of motion translate into symmetries of the Floquet operator. The presence of any of these symmetries results in a vanishing the time-averaged expectation value of the momentum operator for each Floquet eigenstate: $\langle p \rangle_\alpha = 0$. Thus, if one of the symmetries, $\tilde{S}_a$, $\tilde{S}_b$ (10.11), holds then $\langle p \rangle_\alpha = 0$ for all α. Consequently $J(t_0) = 0$ in this case.

By using the Husimi representation [48,49] we can visualize different eigenstates in the phase space, $\{x, p, \tau\}$ and establish a correspondence between them and the mixed phase space structures for the classical limit (Fig. 10.3).

Since the Schrödinger equation (10.12) is linear, the system maintains a memory of the initial condition for infinite times [50]. The asymptotic current value depends on the initial time, t_0, and on the initial wave function, $\psi(t_0)$. For a given initial wave function, $|\psi\rangle = |0\rangle$, we can assign a unique current value by performing an averaging over the initial time t_0, $J = 1/T \int_0^T J(t_0)\, \mathrm{d}t_0$ [44,45]. Fig. 10.4 shows the dependence of the average

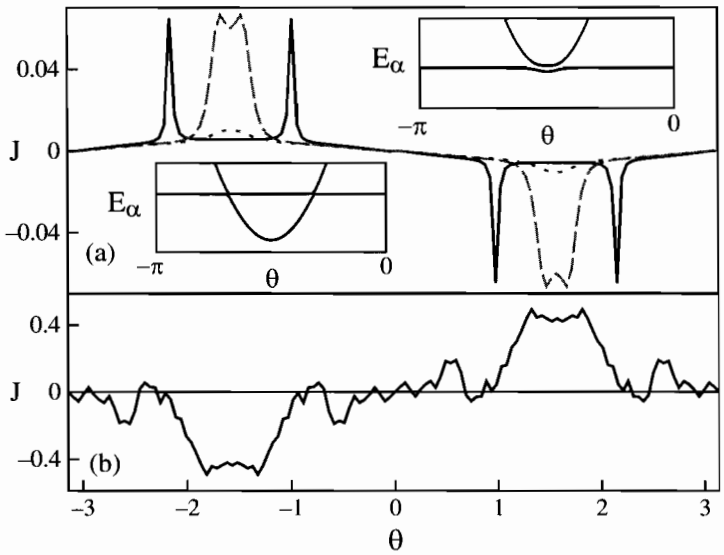

Fig. 10.4. (**a**) The average current J (in units of the recoil momentum) vs. θ for different amplitude values of the second harmonic, E_2: 0.95 (pointed line), 1 (dashed line) and 1.2 (solid line). Insets: relevant details of the quasienergy spectrum versus θ in the resonance region for $E_2 = 1$ (top right) and $E_2 = 1.2$ (bottom left). The parameters are $E_1 = 3.26$ and $\omega = 3$. (**b**) The average current J (in units of the recoil momentum) vs. θ for $E_1 = 3$, $E_2 = 1.5$ and $\omega = 1$

current on the asymmetry parameter θ. Sharp resonant peaks for $E_2 = 1.2$ where the current value changes drastically are associated with interactions between two different Floquet eigenstates. The Husimi distributions show that one state locates in the chaotic layer, and another one in a transporting island. Off resonance the initial state mainly overlaps with the chaotic state, which yields some nonzero, yet small, current. In resonance Floquet states mix, and thus the new eigenstates contain contributions both from the original chaotic state as well as from the regular transporting island state. The Husimi distribution of the mixed state is shown in Fig. 10.3f, the strong asymmetry is clearly observed. The regular island state has a much larger current contribution, resulting in a strong enhancement of the current.

To conclude this section, we would like to emphasize the following two points. For both cases, i.e., the classical and the quantum one, the overall, total current over the whole momentum space is zero [41, 42]. Thus, it is essential to have the initial state prepared localized near the line $p = 0$, because for broad initial distributions the asymptotic current tends to zero. However, if the dynamics is restricted to the lowest band of the periodic potential, no current rectification does occur [51].

10.6 Summary

This surveyed symmetry analysis, originally put forward in Refs. [22,23], provides a general toolbox for the prediction of dynamical regimes for which one can (or cannot) obtain the rectification and directed current phenomenon for a given transport dynamics. First, one has to set up the equations of motions and define a observable (current, magnetization, angular velocity, energy flux, etc.) which should become nonzero, in terms of these dynamical variables. Then, one examines whether there exist transformations (symmetries) which change the sign of the observable and at the same time leave the equations of motion invariant. Upon breaking all the symmetries one can expect the emergence of a non-zero, directed current. This strategy has been successfully tested with Josephson junctions (fluxon directed motion) [52,53] and as well with paramagnetic resonance experiments (spin magnetization by a zero-mean field) [54,55].

Herein, we focused only on the one-dimensional case. By use of more laser beams, experimentalists can fabricate two- and three-dimensional optical potentials [28]. By changing the relative phase between lattice beams, 2D- and 3D-potentials with different symmetries and topologies can be achieved [56, 57]. This fact incites for an extension of the present ratchet studies into higher dimensions.

Moreover, for the phenomenon of Bose-Einstein-condensation (BEC) of cold gases, interactions between atoms become essential and nonlinearities start to play an important role [28]. Many features of BEC dynamics are manifestations of general concepts of nonlinear physics, such as soliton creation and propagation. These collective excitations can then themselves be subjected to a ratchet transport mechanism [58].

References

1. M. von Smoluchowski, Phys. Zeitschrift **XIII**, 1069 (1912)
2. R.P. Feynmann, R.B. Leighton, and M. Sands, *The Feyman Lectures on Physics*, 2nd edn., Addison Wesley, Reading, MA (1963), vol. 1, chap. 46
3. M.O. Magnasco, Phys. Rev. Lett. **71**, 1477 (1993)
4. P. Hänggi and R. Bartussek, Lect. Notes. Phys. **476**, 294 (1996)
5. F. Jülicher, A. Ajdari, and J. Prost, Rev. Mod. Phys. **69**, 1269 (1997)
6. P. Reimann and P. Hänggi, Appl. Phys. A **75**, 169 (2002)
7. P. Reimann, Phys. Rep. **361**, 57 (2002)
8. R.D. Astumian and P. Hänggi, Physics Today **55**, 33 (2002)
9. P. Hänggi, F. Marchesoni, and F. Nori, Ann. Phys. **14**, 51 (2005)
10. B. Norden, Y. Zolotaryuk, P.L. Christiansen, and A.V. Zolotaryuk, Phys. Rev. E **65**, 011110 (2002)
11. P. Reimann, M. Grifoni, and P. Hänggi, Phys. Rev. Lett. **79**, 10 (1997)
12. I. Goychuk, M. Grifoni, and P. Hänggi, Phys. Rev. Lett. **81**, 649 (1998); ibid **81**, 2837 (1998) (erratum)

13. I. Goychuk and Hänggi, Europhys. Lett. **43**, 503 (1998)
14. J. Lehmann, S. Kohler, P. Hänggi, and A. Nitzan, Phys. Rev. Lett. **88**, 228305 (2002)
15. M. Grifoni, M.S. Ferreira, J. Peguiron, and J.B. Majer, Phys. Rev. Lett. **89**, 146801 (2002)
16. H. Linke, T.E. Humphrey, A. Löfgren, A.O. Sushkov, R. Newbury, R.P. Taylor, and P. Omling, Science **286**, 2314 (1999)
17. J.B. Majer, J. Peguiron, M. Grifoni, M. Trusveld, and J.E. Mooij, Phys. Rev. Lett. **90**, 056802 (2003)
18. R. Kubo, J. Phys. Soc. Jpn. **12**, 570 (1957)
19. R. Kubo, N. Toda, and N. Hashitsume, *Statistical Physics II*, Springer, Berlin (1985)
20. P. Hänggi and H. Thomas, Phys. Rep. **88**, 207 (1982)
21. N.G. van Kampen, Phys. Norv. **5**, 279 (1971)
22. S. Flach, O. Yevtushenko, and Y. Zolotaryuk, Phys. Rev. Lett. **84**, 2358 (2000)
23. S. Denisov, S. Flach, A.A. Ovchinnikov, O. Yevtushenko, and Y. Zolotaryuk, Phys. Rev. E **66**, 041104 (2002)
24. P. Jung, J.G. Kissner, and P. Hänggi, Phys. Rev. Lett. **76**, 3436 (1996)
25. O. Yevtushenko, S. Flach, Y. Zolotaryuk, and A.A. Ovchinnikov, Europhys. Lett. **54**, 141 (2001)
26. S. Denisov and S. Flach, Phys. Rev. E **64**, 056236 (2001)
27. L. Guidoni and P. Verkerk, J. Opt. B **1**, R23 (1999)
28. O. Morsch and M. Oberthaler, Rev. Mod. Phys. **78**, 179 (2006)
29. M. Schiavoni, L. Sanchez-Palencia, F. Renzoni, and G. Grynberg, Phys. Rev. Lett. **90**, 094101 (2003)
30. P.H. Jones, M. Goonasekera, and F. Renzoni, Phys. Rev. Lett. **93**, 073904 (2004)
31. R. Gommers, S. Bergamini, and F. Renzoni, Phys. Rev. Lett. **95**, 073003 (2005)
32. R. Gommers, S. Denisov, and F. Renzoni, Phys. Rev. Lett. **96**, 240604 (2006)
33. G. Ritt, C. Geckeler, T. Salger, G. Cennini, and M. Weitz, Phys. Rev. A **74**, 063622 (2006)
34. R.J. Gordon and S.A. Rice, Ann. Rev. Phys. Chem. **48**, 601 (1997)
35. S. Denisov, J. Klafter, and M. Urbakh, Phys. Rev. E **66**, 046203 (2002)
36. S. Savel'ev, F. Marchesoni, P. Hänggi, and F. Nori, Europhys. Lett. **67**, 179 (2004)
37. S. Savel'ev, F. Marchesoni, P. Hänggi, and F. Nori, Phys. Rev. E **70**, 066109 (2004)
38. E. Neumann and A. Pikovsky, Eur. Phys. J. B **26**, 219 (1995)
39. S. Flach and S. Denisov, Acta Phys. Pol. B **35**, 1437 (2004)
40. G.M. Zaslavsky, *Physics of chaos in Hamiltonian systems*, Imperial College Press (1998)
41. H. Schanz, M.-F. Otto, R. Ketzmerick, and T. Dittrich, Phys. Rev. Lett. **87**, 070601 (2001)
42. H. Schanz, T. Dittrich, and R. Ketzmerick, Phys. Rev. E **71**, 026228 (2005)
43. S. Denisov, S. Flach, and P. Hänggi, Europhys. Lett. **74**, 588 (2006)
44. S. Denisov, L. Morales-Molina, S. Flach, and P. Hänggi, Phys. Rev. A **75**, 063424 (2007)
45. S. Denisov, L. Morales-Molina, and S. Flach, Europhys. Lett. **79**, 10007 (2007)
46. J. Gong, D. Poletti, and P. Hänggi, Phys. Rev. A **75**, 033602 (2007)

47. M. Grifoni and P. Hänggi, Phys. Rep. **304**, 279 (1998)
48. K. Husimi, Proc. Phys. Math. Soc. Japan **22**, 264 (1940)
49. K. Takahashi and N. Saito, Phys. Rev. Lett. **55**, 645 (1985)
50. F. Haake, *Quantum signature of chaos*, Springer-Verlag, London (1991)
51. I. Goychuk and Hänggi, J. Phys. Chem. B **105**, 6642 (2001)
52. S. Flach, Y. Zolotaryuk, A.E. Miroshnichenko, and M.V. Fistul, Phys. Rev. Lett. **88**, 184101 (2002)
53. A.V. Ustinov, C. Coqui, A. Kemp, Y. Zolotaryuk, and M. Salerno, Phys. Rev. Lett. **93**, 087001 (2004)
54. S. Flach, and A.A. Ovchinnikov, Physica A **292**, 268 (2001)
55. E. Arimondo, Ann. Phys. **3**, 425 (1968)
56. M. Greiner, I. Bloch, O.Mandel, T.W. Hänsch, and T. Esslinger, Phys. Rev. Lett. **87**, 160405 (2001)
57. L. Santos, M.A. Baranov, J.I. Cirac, H.-U. Everts, H. Fehrmann, and M. Lewenstein, Phys. Rev. Lett. **93**, 030601 (2004)
58. A.V. Gorbach, S. Denisov, and S. Flach, Opt. Lett. **31**, 1702 (2006)